ISSN 0023-1584, Kinetics and Catalysis, 2007, Vol. 48, No. 4, pp. 464–468. © MAIK "Nauka/Interperiodica" (Russia), 2007.
Original Russian Text © I.V. Koptyug, A.A. Lysova, V.N. Parmon, R.Z. Sagdeev, 2007, published in Kinetika i Kataliz, 2007, Vol. 48, No. 4, pp. 493–498.

MECHANISMS OF CATALYTIC REACTIONS

Multinuclear Magnetic Resonance Imaging in Catalytic Research: Recent Advances and Future Prospects

I. V. Koptyug[a], A. A. Lysova[a], V. N. Parmon[b], and R. Z. Sagdeev[a]

[a] *International Tomography Center, Novosibirsk, 630090 Russia*

[b] *Boreskov Institute of Catalysis, Siberian Branch, Russian Academy of Sciences, Novosibirsk, 630090 Russia*

e-mail: koptyug@tomo.nsc.ru

Received June 26, 2006

Abstract—The most important applications of magnetic resonance imaging in catalysis and related areas are considered. In combination with other advanced instrumental methods, this technique can provide essential information about the properties of catalysts and reactors and about processes occurring there. The examples given in the report include the preparation and characterization of porous supports; loading of supports with an active component by impregnation; and investigation of the structure of a granular catalyst bed, various mass transfer processes, and the operation dynamics of a model reactor.

DOI: 10.1134/S0023158407040027

NMR spectroscopy is widely used in catalytic research [1, 2]. However, the useful information provided by this method is averaged throughout the sample. This prevents the researcher from observing any structural inhomogeneity or local features of the processes occurring in the sample. The creation and development of the magnetic resonance imaging (MRI) method have eliminated these limitations and have enabled the researcher to examine objects and processes at a spatial resolution of tens or hundreds of microns [3]. Other advantages of this method are that it is nondestructive, requires no probe or sensor to be introduced into the sample, and is chemically specific. The most important advantage of MRI is that it provides a wide variety of information, both qualitative and quantitative, about objects and processes [4–6]. In particular, MRI is used in the spatial mapping of diffusion coefficients, flow velocity, chemical composition, pore size, temperature, etc. Therefore, MRI is not a single tool, but a universal toolkit applicable to a wide variety of macroscopically inhomogeneous objects and dynamic processes. This makes MRI very promising for chemical engineering and catalysis. As a consequence, there has been keen interest in these applications in recent years [7]. However, they have not become quite common as yet and not all of them have received proper attention.

Various porous materials are frequently used as heterogeneous catalysts and supports. MRI can be used to detect structural inhomogeneities in porous pellets [8]. For this purpose, the pellets are usually saturated with a proton-containing liquid (water, cyclohexane, etc.) to obtain a suitable NMR signal. The resulting images reflect the macroscopic structural features of the pellets, such as cavities and layered structure. Supports are often shaped by wet extrusion. Here, MRI can be used to study extrusion itself [9], to visualize the extrudate morphology [10], and to monitor the moisture content of the pellets during their slow drying in a humid atmosphere [11].

In spite of its comparatively low (micron-scale) resolving power, MRI is applicable to the determination of the size and size distribution of mesopores and macropores. A variety of MRI techniques have been devised for this purpose. In particular, relaxation porosimetry is based on the sensitivity of the nuclear spin relaxation time of the liquid filling a pore to the size of this pore. This sensitivity is due to the fact that the nucleus of a molecule interacting with a solid surface relaxes at a higher rate. This allows the pore surface-to-volume ratio (S/V) to be determined. In the limit of small displacements, the diffusion coefficient of molecules in a pore is a linear function of S/V. Therefore, measuring the diffusion coefficients of liquids and gases in porous materials by pulsed field gradient NMR can also be used in pore sizing. Finally, an NMR cryoporosimetry technique [12] has been devised, which is based on the fact that, according to the Gibbs–Thompson equation, the freezing point of a liquid in a pore decreases as the size of the pore decreases. The frozen liquid does not contribute to the NMR signal. Therefore, by measuring the integrated intensity of the NMR signal while raising (or lowering) the temperature, it is possible to determine the integral pore-size distribution.

Increasing attention is being attracted by gas-phase MRI [13, 14]. Gas adsorption on porous materials allows the problem of the low sensitivity of gas-phase NMR to be solved in part. Furthermore, from NMR measurements taken at different pressures, it is possible

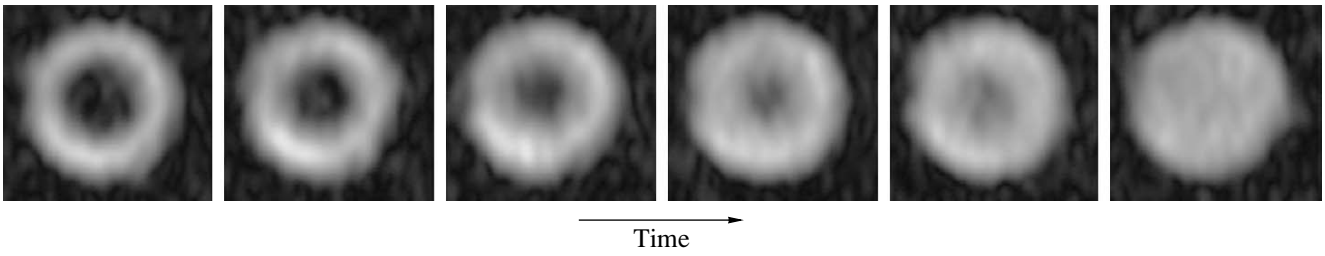

Fig. 1. Dynamics of phosphate transport in a γ-Al_2O_3 pellet placed in aqueous H_3PO_4. The images were obtained by ^{31}P NMR 65, 117, 194, 324, 370, and 1100 min after the beginning of the process. The H_3PO_4 concentration in the solution is 0.76 mol/l; pellet diameter, 3.2 mm; spatial resolution, 172×371 μm; imaging time, 8 min 38 s per image.

to derive gas adsorption isotherms, as was demonstrated by the example of fluorine-containing gases [15]. The sensitivity of gas-phase MRI as applied to inert gases (^{129}Xe and ^{3}He) can be enhanced by 4 orders of magnitude or more by laser-induced gas polarization. This technique helps eliminate some other limitations inherent in gas-phase MRI. For example, it enables one to conduct NMR experiments in very weak magnetic fields and to obtain images from objects in metallic containers [16]. Furthermore, the chemical shift of ^{129}Xe is very sensitive to the chemical environment of the nucleus, and, therefore, ^{129}Xe is an extraordinarily promising molecular probe for characterization of porous materials and for investigation of processes therein [17, 18]. Now we are looking into the possibility of applying multinuclear MRI to the study of the preparation of supported catalysts by impregnation [19]. As an example, we chose the preparation of the phosphate-promoted hydrodesulfurization catalyst (Co)MoS_2/Al_2O_3. Initially, we studied phosphate transport in an alumina pellet placed in an aqueous H_3PO_4 solution. By ^{31}P NMR imaging, we visualized the dynamics of the transport of dissolved phosphate into the pellet bulk (Fig. 1) and demonstrated that the phosphate ion interacts strongly with the alumina surface. Furthermore, after the pellet was dried, ^{31}P NMR imaging enabled us to elucidate the spatial distribution of adsorbed phosphate in the pellet and thus establish a correlation between the phosphate concentration in the solution and the distribution of adsorbed phosphate. The cobalt ion is paramagnetic, and its presence in the solution markedly shortens the relaxation times of the nuclear spins of water. This allowed us to observe cobalt transport in the incipient-wetness impregnation of the pellet with an aqueous cobalt nitrate solution. On addition of citric acid to the solution, it is possible to observe the competing sorption of two compounds. This process results in citric acid displacing cobalt from the outer regions into the pellet bulk. It is noteworthy that impregnating the pellet with an ammonium heptamolybdate solution leads to a longer water relaxation time and it is, therefore, possible to observe molybdenum transport during the impregnation procedure. A similar effect takes place during the impregnation of alumina with $PtCl_6^{2-}$ and $PdCl_4^{2-}$ [20], and, again, it is possible to monitor the transport dynamics of these species during the impregnation process. We have recently demonstrated that it is possible to directly visualize platinum by recording the ^{195}Pt NMR signal [19].

In a number of studies, MRI was used to investigate the deactivation of catalyst pellets caused by coking and the regeneration of deactivated catalysts [21–23]. Solid-phase MRI techniques derive images of coke distribution in a pellet from the NMR signals of the protons of the coke itself [22]. More common MRI techniques are based on the saturation of the coked catalyst pellet with a liquid or on gas adsorption [21, 23]. In particular, it was demonstrated that coke is nonuniformly distributed in pellets and that the extent of deactivation of a pellet depends on the position of this pellet in the reactor.

MRI is also used in the study of granular catalyst beds. The granular bed to be examined is usually saturated with a liquid. Since a liquid in the intergranular space and the same liquid in granule pores have essentially different relaxation times, they can be distinguished by MRI. This allows a 3D image of the granular bed to be obtained and specific structural features of the bed to be revealed. In particular, familiar radial oscillations of bed voidage near the reactor walls were observed [24, 25]. It has recently been demonstrated that solid-phase multinuclear MRI can be carried out with standard liquid-phase equipment [26, 27]. Using NMR signals from a number of quadrupolar nuclei, we obtained 2D and 3D images of cordierite (^{27}Al), alumina (^{27}Al), vanadium oxide (^{51}V), ammonium heptamolybdate (^{95}Mo), glass (^{11}B, ^{23}Na, ^{27}Al, ^{29}Si), etc. By way of example, we present, in Fig. 2, an image of a fragment of an alumina honeycomb monolith support whose channels are filled with vanadium oxide powder. In this case, recording the ^{27}Al signal affords an image of the monolith walls and recording the ^{51}V signal gives an image of the vanadium oxide powder. The direct imaging of solids extended the scope of MRI to the structural and other properties of solid materials.

One of the most fruitful applications of MRI is investigation of mass transport in various systems [3] ranging from pipe flow to filtration in porous materials.

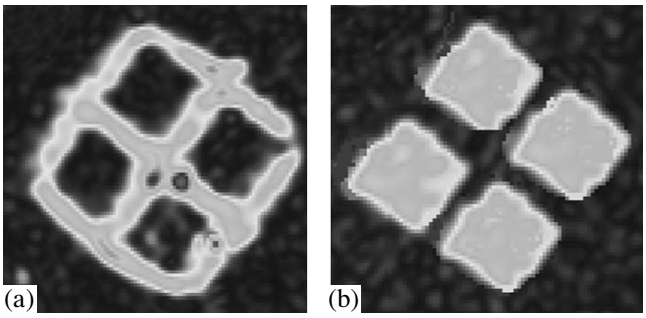

Fig. 2. 2D images of a fragment of a honeycomb γ-Al_2O_3 monolith whose channels are filled with V_2O_5 powder; (a) ^{27}Al and (b) ^{51}V NMR data. The diagonal dimension of the cross section of the fragment is 6 mm. The spatial resolution is 288×288 μm. The imaging time is (a) 17 min and (b) 9 h.

An obvious advantage of MRI is that a single experiment can provide information concerning both the structure and the transport processes. This allows a correlation to be established between the channel or pore structure and transport parameters. For example, the liquid flow velocity field in a granular bed or a fibrous-bed reactor reflects both the bed packing parameters and the flow regime. This makes it possible to determine the magnitude and direction of the velocity vector for each element of the image [28]. There have been studies of multiphase liquid–gas flows with dynamic visualization of the gas and the liquid in granular beds and honeycomb monolith supports [25, 29]. It was demonstrated that velocity fields can also be determined for laminar and turbulent gas flows [30, 31].

In the study of filtration, it is not always possible to achieve a spatial resolution sufficient for obtaining reliable velocity field data. In this case, the pulsed field gradient NMR technique can be employed, which is conventionally used in the study of diffusion processes. For filtration, this technique provides molecular velocity distribution data (more rigorously, the displacement distribution function for a given time interval) [3]. From these data, one can derive the mean filtration rate, the axial and radial dispersion coefficients, and other filtration parameters. This method is applicable to the filtration and other kinds of transport of not only liquids, but also gases and granular solids [32–34], as well as to transport processes in fluidized and bubbling beds [35, 36].

Furthermore, we used the MRI technique in the study of other kinds of matter transport. For example, liquid transport in the drying of wet porous materials, water vapor sorption by selective sorbents of the salt-in-porous-matrix type [37], and the capillary imbibition of moisture were investigated by successive multiple imaging of the distribution of the liquid phase in the porous matrix.

The most interesting application of MRI is probably investigation of catalytic processes in situ. In this case, MRI provides information about the states of the catalyst and the reactor and about the processes occurring there just during the catalytic reaction. The interplay between the chemical reaction, heat and mass transfer, and phase transitions often causes radical changes in the situation. Therefore, data characterizing the liquid phase distribution, the flow velocity, the mass transfer rate, and other process parameters in the absence of a chemical reaction often do not provide a complete understanding of the processes occurring in the reactor during a chemical reaction. The MRI technique can greatly help to remedy this situation. In particular, this is true for investigation of liquid phase distribution in multiphase (gas–liquid–solid) reactors, including the reactor as a whole and individual catalyst pellets. In order to illustrate the potential of MRI in this area, we will consider the heterogeneous hydrogenation of unsaturated hydrocarbons (α-methylstyrene (AMS), *n*-heptene-1, and *n*-octene-1) at elevated temperatures on Pt/Al_2O_3 and Pd/Al_2O_3 catalysts. These reactions are often used as model processes and are at the same time of practical significance. To investigate these reactions, we designed a reactor that is compatible with an NMR microimaging instrument and allows the reaction zone temperature to be raised to 100°C without any risk that the expensive NMR equipment may be damaged [7, 38–40]. In the course of the hydrogenation reaction, for the catalyst bed 1 cm in diameter and 3–4 cm in height, the temperature sometimes rose to 250°C. Initially, we obtained images of the distribution of the liquid phase in a single catalyst pellet used to carry out the reaction for various operating regimes of the reactor [39]. In subsequent experiments, we shortened the imaging time from 4.5 to 0.5 min and then to 2–3 s per 2D image. This enabled us to apply, for the first time, the MRI technique to the visualization of dynamic processes in an operating catalytic reactor. For AMS hydrogenation on a single cylindrical catalyst pellet, we discovered regimes in which the liquid front reciprocated along or across the pellet axis under fixed external conditions [40, 41]. These reciprocations, accompanied by pellet temperature oscillations, are evidence that there is a complicated, nonlinear-law interplay between the chemical reaction and mass transfer. The most significant features of this behavior were later reproduced by simulation taking into account mass transfer, phase transitions, and the chemical reaction [42].

We carried out a similar experiment for a fixed-bed catalytic reactor, varying the diameter of the catalyst pellets. The liquid reactant was fed through a capillary onto the top of the bed at various rates. The distribution of the liquid in the catalyst bed was imaged during the reaction. These experiments demonstrated that, even in a regularly packed catalyst bed, the liquid phase distribution may be extremely nonuniform. Furthermore, if the feeding of the liquid reactant into the reactor is stopped and then resumed, the steady-state distribution of the liquid will be changed [43]. For a pellet diameter of 4–5 mm and a reactor diameter of ~10 mm, the images clearly demonstrated the existence of partially

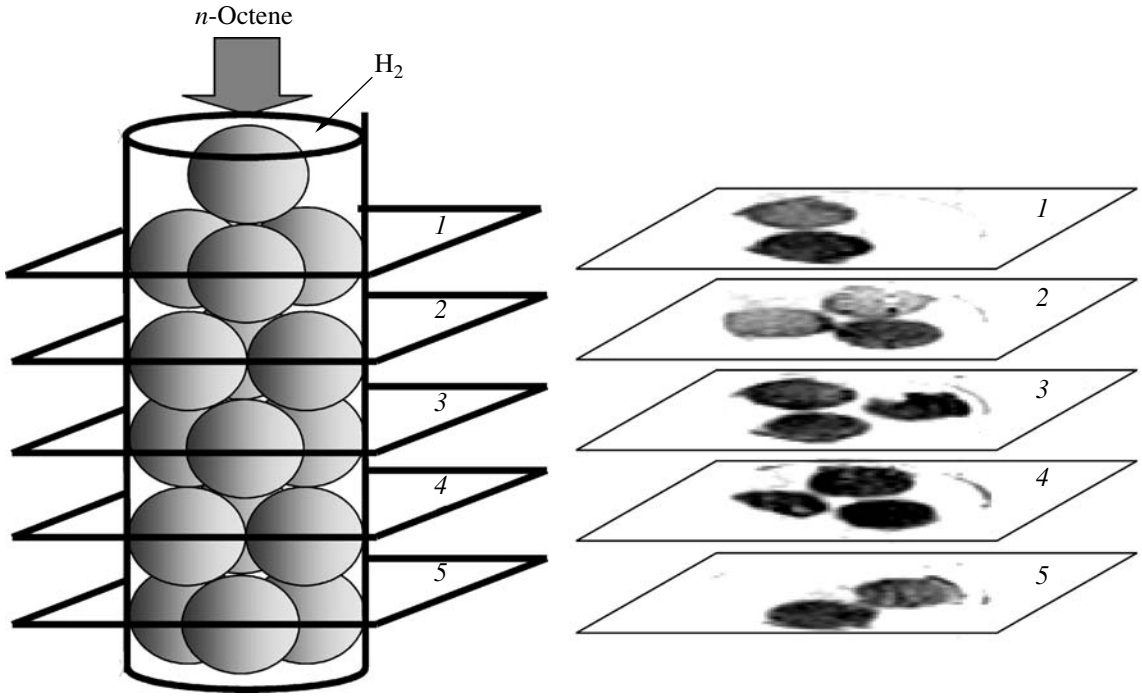

Fig. 3. 2D images illustrating the distribution of the liquid phase in a regularly packed Pd/Al_2O_3 bed during *n*-octene hydrogenation (^1H NMR data). The pellet diameter is 4.2 mm; spatial resolution, 180×310 μm; imaging time, 3 s per image.

wetted and entirely dry pellets in the operating reactor and indicated the ignition of individual pellets and of the entire bed. Figure 3 shows images obtained for a bed consisting of 15 spherical pellets arranged in five three-pellet horizontal layers. One inert pellet (support containing no catalyst) was placed on the top of the bed and served as a liquid reactant distributor. The images presented in Fig. 3 indicate the ignition of single pellets in the top layer and in the lowest two layers. Because this MRI experiment visualized only the liquid phase, the dry pellets and the dry parts of pellets are missing from the images. One pellet in the fourth layer is partially filled with the liquid taken up from its neighbors. Experiments demonstrated that this situation can persist for a long time and be accompanied by reciprocations of the liquid front in the pellet, as in the above-described case of a single pellet. This is evidence of interplay between mass transfer, heat transfer, phase transitions, and the chemical reaction. Obviously, this interplay can be observed only in situ, i.e., in an operating reactor. When there is no reaction, capillary action causes a rapid redistribution of the liquid in the pellet to establish a uniform liquid distribution. The pellets partially filled with liquid, which are observed by MRI, must be the most active in the hydrogenation of the substrate. They contain considerable amounts of the rapidly evaporating reactant and have large dry surface areas, on which reactant vapor is rapidly hydrogenated. It follows from the above data that the phase equilibrium can be disturbed locally during an exothermic reaction to provide conditions favoring the development of critical phenomena in the operating reactor.

Since NMR is a powerful spectroscopic method, combining NMR and MRI can afford spatially resolved conversion data for an operating reactor. This technique was applied to the hydrogenation of AMS [7, 40] and octene [44] and to an esterification reaction [45, 46]. At present, increasing attention is being attracted by the application of MRI to film bioreactors [47].

ACKNOWLEDGMENTS

This work was supported by the Russian Foundation for Basic Research (grant no. 05-03-32472), CRDF (grant no. RU-C1-2581-NO-04), the Chemistry and Materials Science Division of the Russian Academy of Sciences (program nos. 5.1.1 and 5.2.3), the Siberian Branch of the Russian Academy of Sciences (integration project #11), and the RF President's program "Support to Leading Scientific Schools of Russia" (grant no. NSh-4821.2006.3).

Lysova is grateful to the Russian Science Support Foundation and the Global Energy Foundation.

REFERENCES

1. Hunger, M. and Wang, W., *Adv. Catal.*, 2006, vol. 50, p. 147.
2. *NMR Techniques in Catalysis*, Bell, A.T. and Pines, A., Eds., New York: Marcel Dekker, 1994.

3. Callaghan, P.T., *Principles of Nuclear Magnetic Resonance Microscopy*, Oxford: Clarendon, 1991.
4. Koptyug, I.V. and Sagdeev, R.Z., *Usp. Khim.*, 2002, vol. 71, p. 672.
5. Koptyug, I.V. and Sagdeev, R.Z., *Usp. Khim.*, 2002, vol. 71, p. 899.
6. Koptyug, I.V. and Sagdeev, R.Z., *Usp. Khim.*, 2003, vol. 72, p. 183.
7. *NMR Imaging in Chemical Engineering*, Stapf, S. and Han, S., Eds., Weinheim: Wiley-VCH, 2006.
8. Timonen, A., Alvila, L., Hirva, P., Pakkanen, T.T., Gross, D., and Lehmann, V., *Appl. Catal., A*, 1995, vol. 129, p. 117.
9. Gotz, J., Kreibich, W., and Peciar, M., *Rheol. Acta.*, 2002, vol. 41, p. 134.
10. Mantle, M.D., Bardsley, M.H., Gladden, L.F., and Bridgwater, J., *Acta Mater.*, 2004, vol. 52, p. 899.
11. Yashnik, S.A., Ismagilov, Z.R., Koptyug, I.V., Andrievskaya, I.P., Matveev, A.V., and Moulijn, J.A., *Catal. Today*, 2005, vol. 105, p. 507.
12. Strange, J.H. and Webber, J.B.W., *Meas. Sci. Technol.*, 1997, vol. 8, p. 555.
13. Lizak, M.J., Conradi, M.S., and Fry, C.G., *J. Magn. Reson.*, 1991, vol. 95, p. 548.
14. Caprihan, A., Clewett, C.F.M., Kuethe, D.O., Fukushima, E., and Glass, S.J., *Magn. Reson. Imaging*, 2001, vol. 19, p. 311.
15. Beyea, S.D., Caprihan, A., Clewett, C.F.M., and Glass, S.J., *Appl. Magn. Reson.*, 2002, vol. 22, p. 175.
16. Mair, R.W. and Walsworth, R.L., *Appl. Magn. Reson.*, 2002, vol. 22, p. 159.
17. Demarquay, J. and Fraissard, J., *Chem. Phys. Lett.*, 1987, vol. 136, p. 314.
18. Moudrakovski, I.L., Lang, S., Ratcliffe, C.I., Simard, B., Santyr, G., and Ripmeester, J.A., *J. Magn. Reson.*, 2000, vol. 144, p. 372.
19. Lysova, A.A., Koptyug, I.V., Sagdeev, R.Z., Parmon, V.N., Bergwerff, J.A., and Weckhuysen, B.M., *J. Am. Chem. Soc.*, 2005, vol. 127, p. 11916.
20. Khitrina, L.Yu., Koptyug, I.V., Pakhomov, N.A., Sagdeev, R.Z., and Parmon, V.N., *J. Phys. Chem. B*, 2000, vol. 104, p. 1966.
21. Cheah, K.Y., Chiaranussati, N., Hollewand, M.P., and Gladden, L.F., *Appl. Catal., A*, 1994, vol. 115, p. 147.
22. Bar, N.-K., Bauer, F., Ruthven, D.M., and Balcom, B.J., *J. Catal.*, 2002, vol. 208, p. 224.
23. Stapf, S., Ren, X., Talnishnikh, E., and Blumich, B., *Magn. Reson. Imaging*, 2005, vol. 23, p. 383.
24. Sederman, A.J., Alexander, P., and Gladden, L.F., *Powder Technol.*, 2001, vol. 117, p. 255.
25. Nguyen, N.L., van Buren, V., von Garnier, A., Hardy, E.H., and Reimert, R., *Chem. Eng. Sci.*, 2005, vol. 60, p. 6289.
26. Koptyug, I.V., Sagdeev, D.R., Gerkema, E., Van As, H., and Sagdeev, R.Z., *J. Magn. Reson.*, 2005, vol. 175, p. 21.
27. Koptyug, I.V. and Lysova, A.A., *Bruker Spin Report*, 2006, vol. 157/158, p. 22.
28. Gladden, L.F., *Top. Catal.*, 2003, vol. 24, p. 19.
29. Gladden, L.F., Lim, M.H.M., Mantle, M.D., Sederman, A.J., and Stitt, E.H., *Catal. Today*, 2003, vol. 79, p. 203.
30. Koptyug, I.V., Altobelli, S.A., Fukushima, E., Matveev, A.V., and Sagdeev, R.Z., *J. Magn. Reson.*, 2000, vol. 147, p. 36.
31. Newling, B., Poirier, C.C., Zhi, Y., Rioux, J.A., Coristine, A.J., Roach, D., and Balcom, B.J., *Phys. Rev. Lett.*, vol. 93, p. 154 503-1.
32. Koptyug, I.V., Ilyina, L.Yu., Matveev, A.V., Sagdeev, R.Z., Parmon, V.N., and Altobelli, S.A., *Catal. Today*, 2001, vol. 69, p. 385.
33. Koptyug, I.V., Matveev, A.V., and Altobelli, S.A., *Appl. Magn. Reson.*, 2002, vol. 22, p. 187.
34. Matveev, A.V., Barysheva, L.V., Koptyug, I.V., Khanaev, V.M., and Noskov, A.S., *Chem. Eng. Sci.*, 2006, vol. 61, p. 2394.
35. Wang, R., Rosen, M.S., Candela, D., Mair, R.W., and Walsworth, R.L., *Magn. Reson. Imaging*, 2005, vol. 23, p. 203.
36. Savelsberg, R., Demco, D.E., Blumich, B., and Stapf, S., *Phys. Rev. E*, 2002, vol. 65, p. 020301-1.
37. Koptyug, I.V., Sagdeev, R.Z., Khitrina, L.Yu., and Parmon, V.N., *Appl. Magn. Reson.*, 2000, vol. 18, p. 13.
38. Koptyug, I.V., Kulikov, A.V., Lysova, A.A., Kirillov, V.A., Sagdeev, R.Z., and Parmon, V.N., *Dokl. Akad. Nauk*, 2002, vol. 385, p. 205 [*Dokl. Phys. Chem.* (Engl. Transl.), vol. 385, p. 158].
39. Koptyug, I.V., Kulikov, A.V., Lysova, A.A., Kirillov, V.A., Parmon, V.N., and Sagdeev, R.Z., *J. Am. Chem. Soc.*, 2002, vol. 124, p. 9684.
40. Koptyug, I.V., Lysova, A.A., Kulikov, A.V., Kirillov, V.A., Parmon, V.N., and Sagdeev, R.Z., *Appl. Catal., A*, 2004, vol. 267, p. 143.
41. Koptyug, I.V., Lysova, A.A., Kulikov, A.V., Kirillov, V.A., Parmon, V.N., and Sagdeev, R.Z., *Magn. Reson. Imaging*, 2005, vol. 23, p. 221.
42. Kirillov, V.A., Koptyug, I.V., Kulikov, A.V., Kuzin, N.A., Lysova, A.A., Shigarov, A.B., and Parmon, V.N., *Teor. Osn. Khim. Tekhnol.*, 2005, vol. 39, p. 27 [*Theor. Found. Chem. Eng.* (Engl. Transl.), vol. 39, p. 24].
43. Kirillov, V.A. and Koptyug, I.V., *Ind. Eng. Chem. Res.*, 2005, vol. 44, p. 9727.
44. Sederman, A.J., Mantle, M.D., Dunckley, C.P., Huang, Z., and Gladden, L.F., *Catal. Lett.*, 2005, vol. 103, p. 1.
45. Yuen, E.H.L., Sederman, A.J., and Gladden, L.F., *Appl. Catal., A*, 2002, vol. 232, p. 29.
46. Kuppers, M., Heine, C., Han, S., Stapf, S., and Blumich, B., *Appl. Magn. Reson.*, 2002, vol. 22, p. 235.
47. Lens, P.N.L. and Hemminga, M.A., *Biodegradation*, 1998, vol. 9, p. 393.